Richmyer-Meshkov and Rayleigh-Taylor Turbulent Mixing Fronts and Instabilities

J.M. Redondo[1,1], G. Garzon[1], V. B. Rozanov[2] and S. Gushkov[2]

[1] Dept. Fisica Aplicada, Univ. Politecnica de Catalunya
B5, Campus Nord, Barcelona E-08034, Spain
[2] FIAN Lebedev Physics Institute. *Russian.Accademy of Sciences.*
Leninskii Pr. 53. 117924, Moscow, Russia.

ABSTRACT

Plume and Jets are released in an enclosed volume of water and depending on the initial and environmental conditions, the global mixing efficiency of the overall process is measured. The behaviour of individual plumes is very different depending on the environmental energy, which is generated by an oscilating grid at the bottom of the tankself-similarity structures that form in the flow and relate them to mixing and stiring. The evolution of the mixing fronts are compared and the topological characteristics of the merging of the plumes and jets are examined for different configurations. Here we present a detailed comparison of a single plume in the centre of the tank, but also discuss the evolution in overall mixing efficiency produced by a line of up to 9 sideways plumes.

INTRODUCTION The relation between fractal analysis and spectral analysis can be very useful to determine the evolution of

scales. Presently the emerging picture of the mixing process is as follows. Initially a pure RT instability

with lengthscale appears, together with the disturbances caused from the initial set-up (Youngs 1989). The

growth and merging of disturbances favors the appearance of several distinct blobs, bubbles or

protuberances which produce shear instabilities on their sides. These sometimes develop further secondary

accelerated and sheared instabilities. After 2/3 of the tank three dimensional effects have broadened the

spectrum of lengthscales widely enough as to have a fractal structure in the visual range with dimensions

ranging between 2.15 and 2.40. Some differences may be detected in the maximum fractal dimension

evolution in time for experiments with different Schmidt or Prandtl numbers as described in Redondo

(1996). The use of a Pseudo Keulegan number allows to relate the mixing ability of a front .

The difference between RT and RM fronts is analyzed in terms of spectral distribution of the scalar and vector fields (volume fraction, velocity and vorticity). Figure 1. Structure of the RM and RT fronts. Information about the mixing can be extracted from the thickening of the edges examined with Laplacian

filters in both the RT and RM simulations, The use of higher moments of the density and velocity differences shows the differences between the more and less active mixing regions, (Linden and Redondo

2002). The RM fronts generally exhibit lower fractal dimensions than comparable RT fronts.

Abstract. Experimental and numerical results on the advance of a mixing or non-mixing front occurring at a density interface due to gravitational acceleration are analyzed considering the fractal and spectral structure of the front. The experimental configurations presented consists on an unstable two layer system held by a removable plate in a box for Rayleigh-Taylor instability driven fronts and a dropping box on rails and shock tube high Mach number impulse across a density interface air/SF6 in the case of Richtmyer-Meshkov instability driven fronts.

The evolution of the turbulent mixing layer and its complex configuration is studied taking into account the dependence on the initial modes at the early stages and its spectral, self-similar information. Most models of the turbulent mixing evolution generated by hydrodynamics instabilities do not include any dependence on initial conditions, but in many relevant physical problems this dependence is very important, for instance, in Inertial Confinement Fusion target implosion. We discuss simple initial conditions with the aid of a Large Eddy Simulation and a numerical model developed at FIAN Lebedev which was compared with results of many simulations. The analysis of Kelvin-Helmholtz, Rayleigh-Taylor,

e-mail – redondo@fa.upc.edu

Richtmyer-Meshkov and of accelerated instabilities is presented locally comparing their structure. These dominant hydrodynamical instabilities are seen to dominate or at least affect the turbulent cascade mixing zone differently under different initial conditions. In Experiments and Simulations alike, multi-fractal and neuron network analysis of the turbulent mixing under RT and RM instabilities are presented and compared discussing the implications.

.

Key words: Turbulent Mixing Fronts, Shocks, Richtmyer-Meshkov instability, Rayleigh-Taylor instability, Multi-fractal analysis.

1. INTRODUCTION

In the context of determining the influence of structure on mixing ability, multi fractal analysis is used to determine the regions of the RM and RT fronts which contribute most to molecular mixing, We compare both experiments and simulations, looking at both the global geometrical and topological characteristic of the fronts and their small scale cascade processes that lead to mixing. We concentrate here in describing some of the techniques used in both RT and RM flows, presenting examples of the experiments and simulations. The objective of this study is the comparison of models and experiments that model adequately describing process of excitation and subsequent evolution of Rayleigh-Taylor instability (RT) and of Richtmyer-Meshkov (RM) instability. These hydro dynamical instabilities are driven by accelerating the mixing region between two fluids of different densities, but much of what can be learnt from a study of the topology of these flows may also be applied to compressible flows and either externally imposed accelerations or the acceleration due to gravity. The analysis presented here includes: Study of excitation and development of hydrodynamic RT and RM driven flows, resulting in formation of a turbulent mixing layer and the re-stratification of this area caused by its subsequent deceleration.

Many experiments and numerical simulations have been investigated in case of two incompressible fluids subject to accelerations, We may consider the RM instability as a limiting case of the RT one when the acceleration is limited in time acting as a Heaviside function or a Dirac delta. We will first revise the Rayleigh-Taylor case and later describe the Richtmyer-Meshkov case, presenting results on the geometrical and fractal structure of both types of dominant instability, in many practical situations both instabilities occur side by side as shown in figure 2 and it is difficult to identify their different accelerations.

The stability of interfaces between two superposed fluids of different density were first studied by Lord Rayleigh[3] and Taylor(1950)[4] for the case when the dense fluid is accelerated towards the less dense fluid, Chandrasekhar (1961)[5]. For inviscid fluids, the interface is always unstable, with the growth rate of the unstable modes increasing as their wavelengths decrease. The instability of the short waves can be reduced by dissipative mechanisms such as surface tension or viscosity, and then linear theory predicts the maximum growth rate to occur at a finite wavelength. For the viscous two-layer case, where the upper layer (density ρ_1) is denser than the lower layer (density ρ_2), the wavelength λ_μ of maximum growth is

where ν is the mean kinematic viscosity of the two layers and g is the acceleration of gravity. The corresponding maximum growth rate has been described in Redondo and Linden(1990)[6] and Linden and Redondo(1991)[7].

Sharp(1984) characterized the development of the instability through three stages before breaking up into chaotic turbulent mixing. I) A perturbation of wavelength λ_μ grows exponentially with growth rate n_μ. II) When this perturbation reaches a height of approximately ½ λ_μ, the growth rate decreases and larger structures appear. III) When the scale of dominant structures continues to increase and memory of the initial conditions is supposedly lost; viscosity does not affect the latter growth of the large structures.

The advance of a Rayleigh-Taylor front is described in Linden & Redondo (1991)[7], and may be shown to follow $\delta = 2cA\tau^2$ where δ is the width of the growing region of instability, g is the gravitational acceleration and A is the Atwood number defined as $A = \frac{\rho_1 - \rho_2}{\rho_1 + \rho_2}$ .This result concerning the independence of the large amplitude structures on the initial conditions has led to consider that the width of the mixing region depends only on ρ_1, ρ_2, g and time, t-t_0. Then dimensional analysis may be used defining the relevant reduced acceleration driven time with respect to the height of the experimental box, H as:

$$\tau = (t - t_0)\sqrt{H/2gA}$$

The proportionality factor c is considered to be a (supposedly universal) constant, although some dependence with the Atwood number and the initial conditions of the plate removal or random numerical fluctuations is expected (Castilla and Redondo 1994)[11], the key factor is the ratio of the potential and kinetic energy produced by the initial conditions to the Available potential energy of the whole mixing process, if this factor is small, then c tends to a constant value of 0.3, otherwise it will strongly depend on initial conditions and forcing scale. The value of the constant c, has been investigated experimentally and its value for experiments at different values of the Atwood number, A, do not show large variations, with a limit clearly seen for the larger A

experiments performed. Values of c previously obtained experimentally have been in the range (0.03 – 0.035) Read(1984)[9]and Youngs(1984)[10] in experiments with three dimensional effects and large density differences between the two fluids, $A \geq 1.5$. Redondo and Linden[6] measured c for values of A in the range $1x10^{-4}$ to $5.0x10^{-2}$ and found values of $c = 0.035 \pm 0.005$. Numerical calculations in two dimensions[10] gave values of c in the range 0.02 – 0.025. The lesser values[9] have been explained in terms of two dimensional effects inhibiting the growth of the large scale, other experiments and simulations were described in Burrows et al.[12] and Youngs[13,14]. Redondo and Garzon(2004)[15] described further the experiments on Rayleigh-Taylor mixing and the simulations using FLUENT in the Large Eddy Simulation small scale parameterization mode, Following a similar Fractal analysis we will present the results for the RM experiments and simulations. See the figures in Linden et al.(1994)[16] for sequences of the advance of the mixing front experiments, using the non-dimensional time described above, after 3-4 non-dimensional timescales the RT front reaches the ends of the tank. We will describe next some RT and RM experiments both in shock tubes and in a drop apparatus, in section 3 we will describe further the fractal analysis used to perform self similar scaling on the experiments. In section 4 we will repeat the analysis on a series of simulations on RT and RM flows performed at the FIAN Lebedev institute and at UPC and finally we will compare the experiments and numerical results leading to the conclusions.

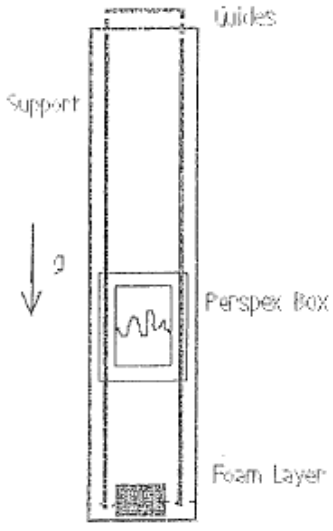

Figure 3: Set up of the Apparatus used for RM drop experiments

at UPC Barcelona and at Arizona University

2. LABORATORY EXPERIMENTS IN RAYLEIGH-TAYLOR AND RIGHTMYER-MESHKOV FLOWS.

Experimental and numerical results on the advance of a mixing or non-mixing front occurring at a density interface due to a sudden acceleration shock are analyzed considering the fractal structure of the front. The experimental configuration consists on a free falling box, where previously a stable sharp density interface has been formed using different fluid combinations between, alcohol water, brine, oil, mercury, and air. The initial density difference is characterized by the Atwood number. The evolution of the Richmyer-Meshkov instability is also here non dimensionalized as $\tau = t/T = t\ (A\ g\ /\ H)^{-1/2}$, with H the height of the box, but also as by $\tau = k\ Vo\ t$, As the free falling box is suddenly stopped, an upwards acceleration, generates a combination of sharp spikes and bubbles, which reach a maximum, function of the Atwood number, and the mixing efficiency at the front.

Richtmyer-Meshkov instability occurs when the interface separating two fluids of different density is accelerated. It may be considered as a type of Rayleigh-Taylor instability when the acceleration is a shock, with a Dirac delta appearance.

The first experiments were done investigating the passage of a shock through a flame front. Richtmyer[17] in 1960 applied Taylor's [4] theory to a sharp acceleration.

Supposing small perturbations ζ produced by a velocity jump ΔV occurring over ΔV for wavelengths k, these perturbations grow, according to equation

$$\frac{d\zeta}{dt} = k\,A\,\Delta V\,\zeta_o$$

being ζ_o the initial interface perturbations and A the Atwood number, i.e. the density difference divided by their sum. Integrating the equation predicts a linear growth in time for the sudden accelerated mixing fronts. Experimental verification of the theory was first provided by Meshkov (1969)[18] in a horizontal shock tube using several gas pairs. Further experiments have been done in shock tubes by Aleshin et al.[19], Valerio et al.[20] Houas and Chemouni[21] and other authors[22-25] . Many other experiments are referenced in the Proceedings of 1-10th International Workshops on the Physics of Compressible Turbulent Mixing (IWPCTM) in http://www.damtp.cam.ac.uk/iwpctm9/proceedings/.

In the experiments, image analysis has been used in order to measure the evolution of the initial turbulent entrainment fronts. The growth of the average front as well as the advances of the spike and bubble heads were measured for the different Atwood numbers. We refer also to some quantitative results obtained by further image analysis of the front evolution of the experiments reported by Castilla and Redondo (1993)[11] at the 4th IWPCTM(Cambridge). The velocity structure near the front also showed baroclinic vorticity production, which enhances mixing. The differences between vorticity generation at Richmeyer-Meshkov and Rayleigh- Taylor fronts will be also discussed in the context of determining

the influence of structure on mixing ability. Multi-fractal analysis is used to determine the regions of the front which contribute most to molecular mixing[15] .

Experiments of the same kind were carried out and described for a range of low values of the Atwood number using different execution techniques. Further to the experiments described in[11] we carried out some more simple experiments for a two dimensional case concentrating on the average values of the Atwood number using brine, oil and water. The additional drop experiments were made filling up a plane tank (2 mm in transversal depth) ,280 mm long, and 130 mm wide. The tank is filled up by the denser fluid till half high then by a side facing tube covered with sponge, the less dense fluid is introduced, the filling up is done carefully to avoid any mixing in the preparation phase.

When the tank is filled up, two possibilities exist, either, the flat tank is turned upside down quickly, pivoting on a plane axis held by the rails and then the RT instability is produced, like in the experiments by Andrews(1986)[26]. The experiments were conducted with two layers of equal depth (h=140mm) with a range of Atwood number from 0.033 to 0.11. Other possibility in order to generate RM instability due to sudden deceleration was to let the flat box fall, guided by railings 1 meter, until it was suddenly stopped by a foam of varying thickness, then the upward shock was modelled using the foam thickness *h,* and gravity *g,* to model an upward velocity difference as $\Delta V = Vo = (g\,h)^{1/2}$.

Records of the process were made using high velocity video, then we can analyze the flow carefully using a digital computer program. DigImage, DigiFlow and Imacalc, software. The aim was to compare RT and RM experiments in a similar set up. Other types of RT experiments can be performed in several other ways; for example by a tank which has a removable metal sheet separating a layer of brine from a layer of fresh water below. The two layers are initially at rest, and the experiment is initiated by sliding the metal sheet horizontally through a slit in one end wall of the tank as in Linden and Redondo (1991) or using an improved version of the plate removal system, as discussed in Dalziel and Redondo(1999).

In this way is possible to reach values of Atwood number of the order of 0.0001 (for the same tank dimensions). Lower values cannot be reached because of the need of a sufficiently high Reynolds number during the development of the instability. To obtain very low values of the Atwood number it is necessary to use a much larger tank, so that there is sufficient time before the whole two-layer system overturned and at the same time the appropriate turbulence level can be ensured.

In the experiments on the mixing produced by Rayleigh-Taylor instability between two miscible (or inmiscible) fluids a layer of fluid (fresh water or oil) is placed over a layer of brine and turned upside down the tank stably stratified fluid is produced and the mixing efficiency of the process is measured relating the density to the dye intensity, before and after the experiments. Useful global measurements are the trajectories of motion of the tank averaged centre of the mixing region along the plane tank in time z(t); the amplitudes of the interface separating the mixing region in time, a(t); the thickness of the mixing region $\delta(t)$; the maximum penetration depth of one fluid into another, L(t); The density distribution in vicinity of the centre of the interface within the mixing region, excepting a zone of turbulence.

Figure 5. Spikes formed at an Hg-Air interface under an RM upward shock

Point conductivity measurements were taken when one of the fluids was brine. A refractometer was also used to calibrate the conductivity probe and to measure salt concentration. The output of the conductivity meter was recorded at the same time as the video images using the software on the image sequences at frequencies of 50Hz. Care was taken to calibrate the output of the conductivity probes before and after the experiments for a range of salt concentrations *(from 0.0 7% to 2.5% in weight*). All the experiments were been done at the same temperature (sometimes with a conductivity probes placed in the centre of the tank). The RM front advanced was measured and it was found to be linear in the dimensionless time scale over the range of density differences used before the restoring force of gravity stopped the advance of the bubbles and spikes, On the other hand RT front growth followed clearly a quadratic law in time if a proper virtual origin is chosen (Linden et al. 1994).

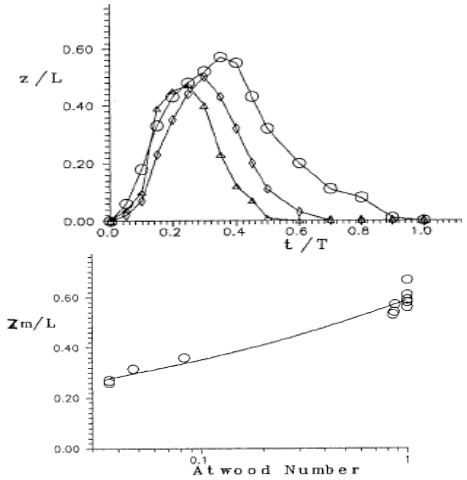

Figure 6. (left) Non dimensional distance advanced by the RM front versus non-dimensional time, t/T. (T= 10 τ) The initial growth, after a delay due to the foam is linear, until restoring gravity reduces the extent of the instabilities, the tails are due to oscillations of the interfaces. Δ indicates water on air experiments, $\Diamond$ oil on air and $\circ$ indicates Hg on air. (right) Variation of the maximum extent of the interface as a function of the Atwood number, for the different substance pairs used to form the interfaces.

Dye visualization was also used to record the advance of both the RM and RT fronts. Small amounts of dye were added to one of the layers and the flow was observed as the instability progressed. Two main results were obtained from an analysis of the images: First the maximum extent, δ, of the inter-penetration region between the two layers, which was measured directly from the video images. Anomalous regions were observed near the sides of the tank, thus the measurements were only taken from the central region, which was insensible at the anomalies due to boundary conditions as well as to the tank dimensions (very small thickness in the case of a 2D Hele-Shaw conditions). Second, by using the calibration of the dye concentration across the tank against known concentrations allowed also to evaluate the average density profiles. The values were obtained by determining the intensity of the light transmitted through the tank, using the image processing system on the digitized video frames. The dye concentration values are integrated across the width of the tank.

An example of the long spikes typical of Atwood numbers near unity is seen in figure 5 when the interface is between Mercury (Hg) and Air. Figure 6 shows the evolution of the spikes in time as they are suddenly accelerated upward and the maximum extent of the spike before the restoring force of gravity stops the growth or the RM instability. Figure 7 shows a LIF sequence of RM instabilities in a similar, more detailed experiment (Jacobs et al. 1997).

To be able to resolve further the detailed structure of the mixing region, the configuration with a plate removal had to be used (Linden et al 1994), in those experiments the RT flow could also be visualized with higher resolution optics using Laser Induced Fluorescence LIF, with a thin sheet of laser light (0,5-1 mm) to illuminate a plane perpendicular to the camera. Thus, elevation views were obtained at different resolutions. The edge of the mixing region was clearly demarcated by this technique (using fluoresceine, rhodamine and small concentrations of dye) so images of the small-scale structures were obtained using zooms. The dye amounts were only added in very small quantities so that the dye acts as a passive tracer. The video images were analysed using the automatic image processing systems Digimage, Digiflow and Imacalc.

Figure 7. Evolution of the structure of the RM front at times T=0-43, at τ = 3 the collapse sets in, in the experiments. Jacobs et al.(1997).

The numerical models used to compare the experiments with the growth of the RM instability at the initial stages 0-0,3 T or 0-3 τ, which could be compared with the early stages of a Shock front passing through a density interface plotted in figure 8 are set in table 1.

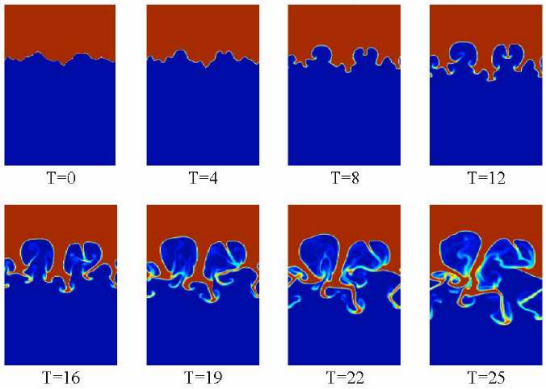

Figure 10. Evolution of the RM front in times T=0, 4, 8, 12,16, 19,22 and 25

Figure 8: Comparison of the RM front in time, in experiments and different models described in Table1

3. RICHTMYER-MESHKOV INDUCED TURBULENCE.

The relation between fractal analysis and spectral Wavelet analysis can be very useful to determine the evolution of scales. Presently the emerging picture of the mixing process is as follows. Initially a pure RT instability with length scale λ_μ appears, together with the disturbances from the plate. The growth and merging of disturbances favours the appearance of several distinct blobs, bubbles or protuberances which produce shear instabilities on their sides. These sometimes develop further secondary shear instabilities. After 2/3 of the tank three dimensional effects have broadened the spectrum of length scales widely enough as to have a fractal structure in the visual range with dimensions ranging between 2.15 and 2.30. Some differences may be detected in the maximum fractal dimension evolution in time for experiments with different Schmidt or Prandtl numbers as described in Redondo (1996).

Figure 9: Side and Plan measures of the maximum fractal dimension of the RT front in time, the plan view is 10 cm from the initial interface, thus the delay of 1.2 τ

In figure 9 the evolution of the maximum fractal dimension of the RT front in the experiments of Linden et al. (1995) both for elevation and plan LIF views is shown.

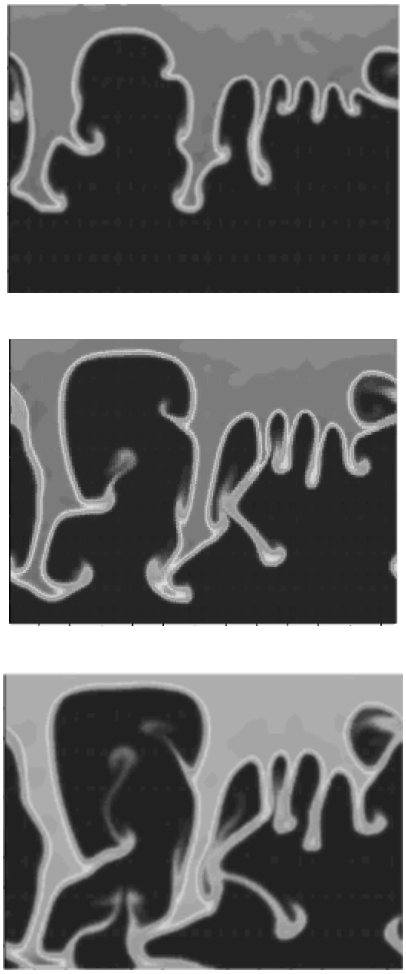

Figure 11: Evolution of the RM front structure.

It is important to note that after 3-4 non dimensional times, the RT front has arrived to the tank extreme and the externally imposed overturning length scale is the size of the tank, after t/T = 3 there is a decrease of the fractal dimension due to the lack of a potential energy input of energy. This effect is normally not modelled in numerical simulations of neither RT nor RM fronts.

Figures 10 and 11 show numerical simulations of the RM fronts, performed at the FIAN Lebedev Physics Institute (Stepanov et al 2004), that clearly show the differences with RT fronts, the spike structure is much more pronounced and the advance of the front is clearly not quadratic, but has a more complex combination of power law dependence. As the dominant effect is a linear time dependence, probably the effect of initial conditions is more important in RM than in RT fronts. Different theoretical arguments will be discussed below but in figure 12 it is clearly shown that the spike head advance has a different law than the smoother concave bubble structures that exhibits a linear growth.

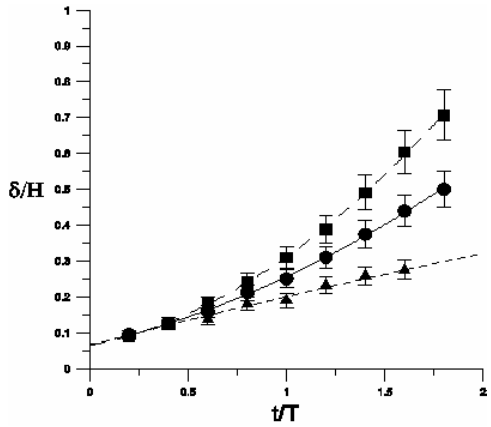

Figure 1: *This is an example of figure. Figure caption is in Times 9 points, italic, justified (centred if it runs shorter than two lines).*

Figure 12: Evolution of the center, (dots), maximum (squares) and minimum (triangles) extents of the evolution of the spike RM front for the different non-dimensional times

It is interesting also to compare the evolution of the thickness of the spikes and of the bubbles, as also seen in the experiments of Castilla and Redondo (figure 5) the spikes are much more narrow, but the simulations show that after 2 non dimensional time scales they seem comparable with a 1 to 10 anisotropic structure, this seems independent on the spectral structure of the initial conditions.

Stepanov et al.(2004) have considered the effect of different initial conditions on the RT and RM front advances using a neuron network analysis of the turbulent mixing. They found a weak dependence of the higher order modes of the initial conditions on the advance of the front and used successfully a mapping based on Kohonen techniques that is used to group in a parameter map the different possible behaviours of the mixing front in terms of the initial conditions. Fractal analysis can also aid in relating front advance, mixing and the highly non-homogeneous mixing that takes place at the front edges.

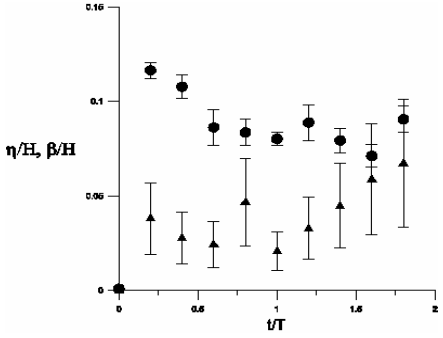

Figure 13: Evolution of the average thickness of the spikes (circles) and bubbles (triangles) of the RM simulation described in figure 11 front comparing experiments (dots) and LES model (squares) and (triangles), The virtual origin is not the same as the initial conditions of the LES were random.

4. LES MODEL OF A RAYLEIGH-TAYLOR MIXING FRONT

Figure 14, shows the evolution of the multifractal dimension (calculated performing the box-counting algorithm) for each level of velocity modulus (a) and volume fraction (b). Much more relevant information can be extracted from these evolutions than from the maximum value presented by Linden et al.(1994), furthermore it is of great interest to study independently the fractal properties of velocity, volume fraction and vorticity fields The fact that the RT front is accelerating is reflected in figure 4a that shows how initially there is a small range of velocities and the regions of higher velocity take some time to develop a fractal structure. It seems that precisely these "fast vortical spots" that lie at the sides of the bubbles and spikes are responsible for most of the transport.

The LES simulations used to model the RT fronts are described fully in Redondo and Garzon (2004) and were obtained using Fluent. The evolutions of the fronts were compared with the experiments of Linden and Redondo (1991) confirming the quadratic dependence of the average front advance, but the aim of this work was to identify the distribution of mixing and the self-similarity of the fronts.

More work is still needed in order to fully interpret the results of the fractal analysis, but it is interesting to compare changes in the fractal dimension with other experimental set ups. Information about the mixing can be extracted from the thickening of the edges due to the phenolphthalein colour change in Linden et al. (1994), or in the numerical simulations, and this thickness can be now analyzed with a digitizer system. For lower density runs with phenolphthalein, it was apparent that the vorticity originated by the plate increased mixing at the central regio of the vortices produced by it. This effect can be avoided using intermediate density differences.

Both in the experiments and in the numerical simulations the fractal evolution that indicates a transition to a turbulent flow is apparent by the increase in the maximum fractal dimension of the interface center (50/50 mixing ratio) between Dm = 1 and 1.4. (see figure 9) The Spectra and fractal aspects of the numerical simulations are compared with the experiments showing agreement in the maximum fractal dimensions only for dimensionless times 1-3. Scatter-plots of the multi-fractal dimension at two different times of the different volume fractions of the front indicates its non-uniform curdling. It was also noticed that the increase in fractal dimensions is not the same for all the levels of volume fraction (or density) nor velocity.

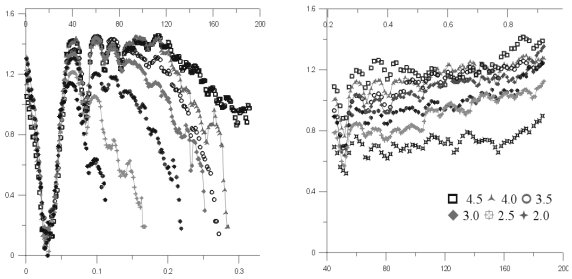

Figure 14: Evolution of the Fractal dimension values for the different values of Velocity (left) and volume fraction (right) in time for the simulation of the RT front.

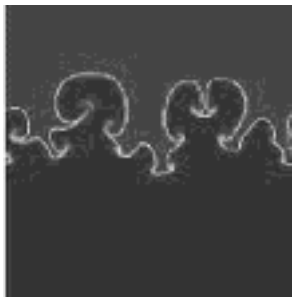

Figure 15: Evolution of the marked interfacial region, where the fractal dimension values for the intermediate volume fraction values for the RT front are higher than in the homogeneous regions.

Figure 14 shows the evolution of the fractal dimensions for each level of the velocity magnitude and of the volume fraction, it is clear as shown previously by Linden et al (1994) the growth in maximum fractal dimension, but using a much more complex multifractal analysis, where each set of values of a different intensity is analized separately using box counting, the mixing structure of the fronts is revealed to be more complex. As the front evolves in time and accelerates, higher velocity values are included in the velocity map structure, but it is interesting to see that the highest fractal dimension values do not correspond to these sparse sets of high velocities, which are typical of the heads of the RT fronts. As shown in figure 14 maximum fractal dimensions occur at values of 0.1 to 0.2 of the maximum velocities. There is a plateau that widens in time where maximum fractal dimensions take place. This would be an indication that most of the self-similarity takes place at the sides of the bubbles instead than at the front head. In figure 15, the 50%

volume fraction isoconcentration values are marked in grey as the RT instability evolves, the increase in complexity is reflected by the increase in maximum fractal dimension values, these points correspond to a pixel intensity of about 120 in the right plot of figure 14, It appears than the velocity structure is more complex (higher fractal values) than the density structure.

The overall evolution of the fractal dimension for different values of the volume fraction or density of the RT front grows in time, but it is interesting to note that the slightly higher values take place at the sets of higher concentration of the density. The vorticity values also show a different fractal dimension evolution as shown by Redondo and Garzon (2004) so that the different sets of measurements (density, velocity, vorticity) exhibit a different cascade structure.

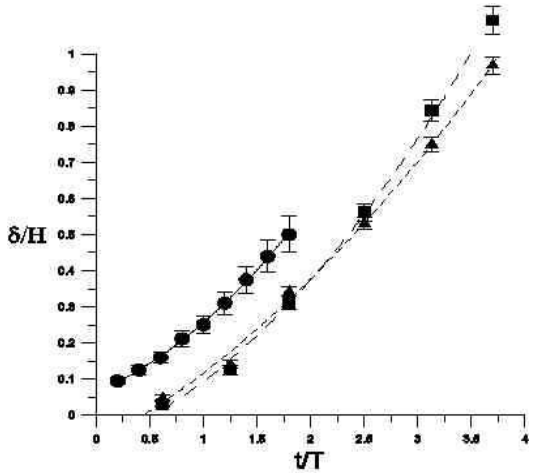

Figure 16: Evolution of the average advance of a RT front comparing experiments (dots) and LES model (squares) and spectral model (triangles), The virtual origin is not the same as the initial conditions of the LES were random.

Figure 16 shows the overall evolution of the RT front both for the experiments of Linden and Redondo(1991) and the simulations of Redondo and Garzon(2004) and Stepanov et al (2004) showing good agreement, except for the virtual origin needed for the experiments.

Experimental and numerical results on the advance of a mixing or non-mixing front occurring at a density interface due to a sudden acceleration shock have been analyzed considering the fractal structure of the fronts as well as several geometrical indicators of the local mixing processes. The experimental configurations compared are several and have been previously described in detail in Linden and Redondo (1991) and Castilla and Redondo (1993) for RM fronts. This later configuration, that has also been employed by Jacobs et al. consists on a free falling box, where previously a stable sharp density interface has been formed using different fluid combinations, alcohol water, oil, mercury, air. The initial density difference is characterized by the Atwood number. The evolution of the Richmeyer-Meshkov instability is non dimensionalized also by τ, As the free falling box is suddenly stopped, an upwards acceleration, generates a combination of sharp spikes and bubbles, which reach a maximum, function of the Atwood number, and the mixing efficiency at the front. A similarity solution may be found, following Youngs(1991). The cuantitative results obtained by image analysis of the front evolution described by Castilla and Redondo (1993) have been explained and compared with numerical simulations, the velocity structure near the front shows the baroclinic vorticity production, which enhances mixing. The differences between vorticity generation at Richmeyer-Meshkov and Rayleigh-Taylor fronts is also interesting due to the different scaling properties between density or volume fraction, velocity and vorticity found by Redondo and Garzon(2004)

More work is still needed in order to interpret the results of the fractal analysis, but it is interesting to compare changes in the fractal dimension with other experiments such as stably stratified turbulence of flame propagation. Information about the mixing can be extracted from the thickening of the edges due to the phenolphtalein colour change in Linden et al(1995), using the technique described in Dalziel and Redondo(2006). This thickness can be now analysed with the digitizer system. For lower density runs with phenolphthalein, it was apparent that the vorticity originated by the plate increased mixing at the centre of the vortices produced by it. This effect can be avoided using intermediate density differences.

Both in the experiments and in the numerical simulations the fractal evolution that indicates a transition to a turbulent flow is apparent as shown by Linden et al(1995) by the increase in the maximum fractal dimension of the interface centre (50/50 mixing ratio) between 1 and 1.4. The relation between fractal analysis and spectral analysis can be very useful to determine the evolution of scales. Presently the emerging picture of the mixing process is as follows. Initially a pure RT instability with lengthscale λm appears, together with the disturbances from the plate. The growth and merging of disturbances favours the appearence of several distinct blobs, bubbles or protuberances which produce shear instabilities on their sides.

These, very often, develop further secondary shear instabilities. After 2/3 of the tank Height three dimensional effects have broadened the spectrum of lengthscales widely enough as to have a fractal structure in the visual range with dimensions ranging between 2.15 and 2.30.

It is important to realize that the body forces acting on the density differences (either gravity or inertial

accelerations in non-Boussinesq flows) may affect turbulence structure as discussed by Redondo(1990) . The effects of these additional terms in Navier-Stokes equations change the topology of the flow and of its scaling, which may be described as a non-homogeneous fractal, this means that there is no unique fractal dimension for the range of length scales possible in the flow, nor for the different density interfaces this is specially true if there are different physical mechanisms at work. Different behaviour would be expected in the inertial-diffusive subrange for Schmidt numbers Sc >> 1 and the anisotropy introduced by Buoyancy or inertial forces will also modify the value of the fractal dimension D.

In analyzing the fractal nature of a stratified interface in either the RT or RM fronts, we have limited the fractal description to length scales comparable with the extent of the fronts. Redondo and Garzon(2004) showed the differences between the heads and the sides of the RT instabilities. In order to compare RT and RM flows, or comparing different types of experiments (i.e. Shock tube fronts, overturning interfaces, convective flows, etc..) it is interesting to non dimensionalize the range of scales with the non-stratified integral length scale of the turbulence, or with a lenthscale related to the local turbulent intensity. The reasons for these choices are : 1) The fact that large scales are most likely to affect the front interfaces, which may be due to wall or experimental asymetries. 2) The easy identification of the integral length scale of the turbulence from velocity data or visual analysis. 3) The effect of the stratification on scales larger than the Buoyancy or the Ozmidov scale. 4) The difficulty in resolving scales near the Kolmogorov length scale, which are generally supposed not to be greatly affected by stratification. Redondo (1990) found that the stable stratification reduces the fractal dimension of the turbulence. The effect of the reduction was to decrease the contact surface between the dense and light fluid across the variable turbulent interface, for very high Richardson number the interface was seen not turbulent anymore, and all that remains is just an Euclidean plane surface. There is a double influence of the stratification on a turbulent density interface, first to reduce the overall vertical displacements by means of an increased transfer of kinetic to potential energy, and from vertical to horizontal length scales.

More detailed experiments will be needed to be able to determine the exact mechanisms which reduce the effective fractal dimension, as well as the effect of higher order geometrical parameters, such as the structure functions, which seem to be relevant in non-homogeneous fluids (Mahjoub et al 1998).

The structure of a blob shows a relatively sharp head with most of the mixing taking place at the sides due to what seems to be shear instability very similar to the Kelvin-Helmholtz instabilities, but with sideways accelerations. The formation of the blobs with their secondary instabilities produces a turbulent cascade, evident just after about 1 non-dimensional time unit, from a virtual time origin that takes into account the linear growth phase, as can be seen by the growth of the fractal dimension in the front in time.

The thickness of the laser sheet was 1-2 mm. which is considerable larger than a typical Kolmogorov length scale, η calculated in terms of a turbulent velocity a tenth of the falling velocity across the depth of the box, or of the RT (or RM) front thickness as

$$u' = \tfrac{1}{10}\sqrt{\delta c g A}$$

and

$$\eta = \left(\frac{\nu^3}{\varepsilon}\right)^{\frac{1}{4}}$$

using that

$$\varepsilon = \frac{u'^3}{\lambda_m}$$

With these equations we find an estimate of 0.01 to 0.4 mm. for η. This means that the minimum scale will be constrained by the thickness of the laser beam, and in principle there is a maximum possible range of scales between the integral length scales and the laser thickness, or the Image pixel resolution.

The box dropping experiment shown allows the study of a considerable range of Atwood numbers 0.3 to almost 1, by using combinations of fluids like either brine and water or Mercury and air. The velocity difference across the interface may be modelled by rising the drop height and the shock duration Δt was varied by using different foam thicknesses at the base of the drop tank. The results of the experiments discussed in Castilla and Redondo(1994) agree with Mikaelian's (1985) growth of the mixing (or instability intermingling region). These experiments show a linear growth on a large ensemble average of experiments following the equation.

$$\delta = 0.14 \Delta V \; A \quad t$$

Individual experiments, on the other hand, show the effect of wave resonances in their growth. In what seems a Non-Linear growth

$$\delta = c \Delta V \; A \quad t^{\frac{2}{3}} ,$$

giving a reasonable fit to some of the slowest growth rates in the experiments, but the restoring effect of gravity, which we have to remember, that is always present in the RM drop experiments prevents further growth. A Damped oscillation of the interface sets in after the shock decays.

Slower front growths of the interface were recorded mostly in the Hg - H_2 O experiments.

The oscillations in the simulation data are the result of the data being obtained from a single vertical plane in a single realisation of the flow. The differences at early time are due in part to the presence of the barrier in the field of view for the experiments. The two plots show a good level of agreement after the barrier is fully withdrawn with both tending towards a k-5/3 slope suggestive of fully developed turbulence.

The apparent differences between the experiments and simulations at early times are largely due to the presence of the barrier in the viewed region. After the barrier is fully removed, both curves tend rapidly towards an approximately constant dimension of D1.45 until the flow starts to interact with the top and bottom boundaries of the tank. At late times there is competition between the dimension increasing due to the formation of more convoluted structures and diffusion smoothing them out.

Ultimately diffusion causes the dimension to return to D=1 with the formation of a stable stratification. The use of ensemble data removes many of the apparent fluctuations and differences between the two data sets. Analysis of the fractal dimension for a range of different concentration contours shows the dimension to be independent of the concentration threshold during the similarity phase where the dimension remains approximately constant.

Table 2

Comparison between Maximum fractal dimension D(i) values for volume fraction

contours for RT and RM instability driven fronts

we have also shown that it is possible to obtain a reasonable model of the real experimental initial conditions found in simple Rayleigh-Taylor experiments. This model consists of a vortex sheet injected by the barrier as it is withdrawn, with potential flow in the body of the tank. By utilising this model as the initial conditions for numerical simulations, it is possible to obtain significantly improved agreement between experimental measurements and numerical predictions of the flow. If the initial conditions are not modelled adequately, then agreement will never be achieved.

The traditional $\delta_1=c_1\, Ag\, t^2$ model for the growth rate of the RT instability is not an adequate description for flows where the initial conditions are in some sense inhomogeneous. While it is clear that a quadratic component remains, there is a spatial dependence in this component in addition to a linear term resulting from the vortex sheet. In these experiments the vortex-driven flow down the right-hand is dominated by a linear growth whereas the flow elsewhere follows the quadratic law much more closely. We therefore recommend that comparisons should not be limited to simply the c_1 constant, but should encompass more details of the growth and internal structure of the flow considering different powers of *t* together with initial conditions.

The absence of a homogeneous quadratic growth suggests that the flow is not fully self-similar over all scales. However, the existence of a $k^{-5/3}$ concentration fluctuation power spectrum and constant fractal dimension indicates that internal similarity is still attained. As is to be expected, this structure changes significantly once the mixing region reaches the top and bottom of the flow domain.

We have presented a series of experiments to investigate the nonlinear evolution of the RT and RM instabilities. For a constant acceleration, the RT instability is found to grow self-similarly. The growth coefficients ai are measured over a comprehensive range of density ratio and the results are found applicable to supernova exlposions. For an impulsive acceleration, there are two components.

The RM impulse from a shock is greatly reduced at high Mach number due to compressive effects in reasonable agreement with linear theory. The ensuing motion is essentially imcompressible describable by a power law. However, the exponents obtained from the compressible RM experiments are larger than those obtained from incompressible RT experiments. The discrepancy is currently not understood.

The effect of non-Newtonian constitutive properties on the RT instability was investigated with scaled experiments of long duration (15/y) and well characterized material properties.

The regions of higher local fractal dimension increase, both in number and with higher values as time evolves for both the RT and the RM experiments until a non-dimensional time of 3-4 after that time the decrease of the RM front is faster than that of the RT.

On the other hand the RM fronts achieve faster a self similar fully turbulent level that corresponds to a fractal dimension of 1.4-1.5 for a wide range of velocities and volume fractions.

This is a sample paper for the "Workshop on Environmental Turbulence, Advances in Turbulence XII summer course – AT 2010". Laboratory experiments will be described here comparing the mixing efficiency and the main flow descriptors, further LES numerical simulations of convective flows are presented in Yague and Redondo(1996), the model solves the Boussinesq set of equations in a two dimensional grid and is based on Rees(1987). Together with the momentum equations, the continuity equation for incompressible flow is used taking into account only x and z components. Initially the subgrid scaling assumed a constant turbulent viscosity defined in terms of dimensional scaling with a simple turbulent parametrization based on local mixing length scales as $\nu = l^2 / \Delta t$ and taking the integral scale initially as a constant in terms of the mesh size as $l = 0.23 (\Delta x \Delta z)^{1/2}$ Different aspect ratios of the convective flow, generated by buoyancy are considered where a complexThe plumes are formed by injecting a dense fluid from a small source (from one to nine orifices) into a stationary body of lighter brime (saline solution) contained in a tank. The source fluid was dyed with fluorescein and we use the LIF technique. The plumes were fully turbulent and we have both momentum and bouyancy regimes. The fractal dimensions of contours of concentration were measured. The fractal analysis of the turbulent convective plumes was performed with the box counting algorithm for different intensities of evolving plume images using the special software Ima_Calc. Fractal dimensions between 1.3 and 1.35 are obtained from box counting methods for free convection and neutral boundary layers. Other results have been published which use the box counting method to analyze images of jet sections – produced from LIF techniques- and determined that the fractal dimension of jet boundaries was 1.36. Our investigations indicate a mean fractal dimension of 1.23 for the one plume experiment.

GENERAL SPECIFICATIONS

Document format

Extended Abstract and Paper length and page size

Maximum paper length is twelve standard A4 (21 x 29,7 cm) pages.

The text area is defined by left, right, top and bottom margins of 2 cm. In no case should the text on any page exceed this text area.

Body text

Body text is in 2-columns, column width is 8,25 cm, margin between columns is 0,5 cm.

Language and font

All manuscripts must be in English.

Use Times, Times Roman or Times New Roman 10 points throughout the text, with simple interline spacing. Spacing between paragraphs is 3 points.

Headings styles

FIRST LEVEL HEADINGS

First level headings are in Times 10 points, cap/lower case, bold aligned on the left-hand border of the column. Leave an extra 10 point space before and after each first level heading.

Second level headings

Second level headings are in Times 10 points, cap/lower case, bold aligned on the left-hand border of the column. Leave an extra 5 point space before and after each second level heading.

Third level headings

Third level headings are in Times 10 points, cap/lower case, italic, underlined, aligned on the left-hand border of the column. Leave an extra 5 point space before and a 3 point space after each third level headings.

FIRST PAGE SPECIFICATIONS

Top of first page

At the top of the first page only : write the colloquium title, date and venue on two lines, Times 9 points, italic, centred across both columns.

Title and authors

Leave a 16 point blank line, and then write the paper title in Times 16 points, bold, cap/lower case, centred across both columns. Leave a 16 point blank line below the title line.

Write author(s) affiliation and addresses in Times 10 points, italic, centred across both columns.

Abstract

Each paper must include an abstract which must be no longer than 200 words and need not to be the same as the previously submitted abstract. Use Times 9 points, italic, fully justified across both columns with 1 cm left and right indents with respect to the borders of the text area.

FIGURES

The legibility of the illustration is crucial. Clearly label each figure and number them consecutively. Cite all illustrations in the text consecutively by writing "Fig. 1 :" or "Figure 1" and place the figure as closed as possible to its first mention in the text, preferably at the top or bottom of a column.

Each illustration must include a caption that clearly and succinctly explains its content. Use Times 9 points, italic for figure caption. The figure caption is positioned just below the figure, centred with the column (or both columns) width, beginning with "***Figure 1***:". If the caption

runs longer than two lines, then justify it full width of the column (or both columns).

Leave a 10 point extra space before the figure, and another 10 point extra space after the caption.

For wider figures, place across both column width and centre within the page width.

If necessary, figures can be also grouped at the end of the paper.

No colour figures or photographs will be accepted.

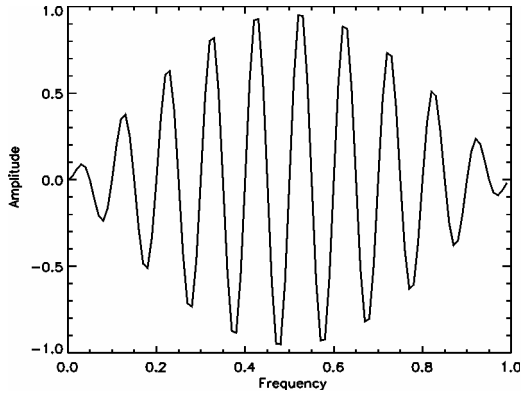

Figure 1: *This is an example of figure. Figure caption is in Times 9 points, italic, justified (centred if it runs shorter than two lines).*

TABLES

The font for the entire table is Times 9 points, including title (footnotes are in Times 8 points). The rules for the position, number and title (caption) of tables are the same as for figures, except that the title is positioned above the table.

Table 1: *This is an example of table. Table title is in Times 9 points, italic, justified (centred if it runs shorter than two lines).*

	First column	**Second column***	**Third column****	**Fourth column**
1st row	100	200	300	400
2nd row	500	600	700	800
3rd row	530	640	750	860
4th row	540	650	750	860

* This is a footnote of the table

** This is a second footnote

EQUATIONS

Equations should be the same point size as the body text (Times 10 points), italic, centred. Place each equation on a separate line and number equation sequentially. Enclose the equation number in parentheses and place it to end at the right-hand margin. Leave a 5 point extra space before and after each equation.

$$\tilde{\rho}(r,t) = A_1^0(\omega r/c)e^{i\omega t} \tag{1}$$

$$p(\mathbf{x},t) = \int \frac{d\mathbf{y}}{4\pi|\mathbf{x}-\mathbf{y}|} d\mathbf{y} \tag{2}$$

$$f(x) = \sum_{i=1}^{\infty} \alpha_n \sin\left(\frac{n\pi x}{l}\right) \tag{3}$$

FOOTNOTES

Footnotes must appear at the bottom of the page where they are cited by superscripts numbers[2]. Place a ½ line long above the foot note. Print the footnote in Times 8 points and keep within the column of occurrence[3].

REFERENCES

Bibliographic references are cited sequentially in square brackets [1] in the body text. The bibliography is listed at the end of the paper in a separate main-headings section. For each bibliographic reference, write the number in square brackets, author and co-authors names, *"Title in Italic,"* book or journal reference and date.

ACKNOWLEDGEMENTS

This work was supported by the European Union: International Science and Technology Centre Project ISTC#1481 "Neuron Network Forecasting of Turbulent Mixing Development Based on Wavelet Analysis" and INTAS and the Spanish Science Ministry grants MCT-FTN2001-2220, ERBIC15-CT96-0111 and Generalitat 2001SGR00221. We would also like to thank for helping with analysis of the data: Drs. Otman B. Mahjoub, Alexei Platonov, and Joan Grau.

BIBLIOGRAPHY

[1] Larchevêque L., Sagaut P., Lê T-H and Comte P. *"Large eddy simulation of a compressible flow in a three dimensional open cavity at high Reynolds number"* Journal of Fluid Mechanics. **516**, 265-301, 2004.

[2] González-Nieto, P. L., Redondo, J. M., Cano, J. L. and Yagüe, C.: 2004, The role of initial conditions on Rayleigh-Taylor mixing efficiency, *International Workshop on The Physics of Compressible Turbulent Mixing,* Ed. Dalziel S., DAMTP, Cambridge University, U.K.

[3] Grau, J. *Instruction manual for ImaCalc, version 1.1.* **UPC**, Barcelona, Spain. 2002.

[4] Redondo, J. M., Grau, J., Platonov, A. And Garzón, G., 2008. Análisis multifractal de procesos autosimilares: imagenes de satélite e inestabilidades baroclinas. Revista Internacional de Métodos Numéricos para Cálculo y Diseño en Ingeniería. **24**, 1. 23-35, CIMNE.

[5] Sykes, R. I. and Gabruk, R. S., 1994. "Fractal representation of turbulent dispersing plumes". Journal of Applied Meteorlogy, vol. 33, pp. 721. 1994.

[6] Prasad, R. R., and Sreenivasan, K. R., 1990. " The measurement ans interpretation of fractal dimension of surfaces in turbulent flows". Phys. Fluids A, 2, 792-807. 1990.

[7] López González-Nieto, P., Cano, J. L. and Redondo, J. M., "Buoyant mixing processes generated in turbulent pluma arrays"

[2] This is a footnote, appearing at the end of the page

[3] This is another footnote.

in Experimental and Modelling Micrometeorology, Física de la Tierra, vol. 19, pp. 205-219, 2007.
[8] Yagüe, C., 1992. *Estudio de la mezcla turbulenta a través de experimentos de laboratorio y datos micrometeorológicos*. Ph. D. Thesis. Complutense University of Madrid.

[9] Linden, P. F., Redondo, J. M. and Caulfield, C. P.: 1992, *Advances in Compressible Turbulent Mixing*, edited by W.P. Dannevik, A.C. Buckingham and C.E. Leith, Princenton University.

[10] Linden, P. F. and Redondo, J. M.: 1991, *"Molecular mixing in Rayleigh-Taylor instability"*. Part I: Global mixing, Phys. Fluids. **A3** (5), 1269-1277.

[11] Harindra J.S. Fernando, *"Turbulent mixing in stratified fluids."* Annu. Rev. Fluid Mech. **23**, 455-493. 1991.

[12] Read, K. I. "*Experimental investigation of turbulent mixing by Rayleigh-Taylor instability"*, *Physica* **12D**, 45-58. 1984.
[13] Linden, P. F., Redondo, J. M. and Youngs, D. L.: 1994, "*Molecular mixing in Rayleigh-Taylor instability",* J. Fluid Mech. **265**, 97-124.
[14] Sharp, D. H. "*An overview of Rayleigh-Taylor instability"*, Physica **12** D, 3-15. 1984
[15] Mahjoub O.B., Redondo J.M. and Babiano A. "*Hyerarchy flux in nonhomogeneous flows" in Turbulent diffusion in the environment* Eds. Redondo J.M. and Babiano A. 249-260. 2000.

[16] Redondo J.M. *"Mixing efficiencies of different kinds of turbulent processes and instabilities, Applications to the environment in Turbulent mixing in geophysical flows"*. Eds. Linden P.F. and Redondo J.M. 131-157. 2002.

[17] Youngs D.L. (1989) .*Modelling turbulent mixing by Rayleigh-Taylor Instability*.. Physica D 37, 270-287.

[18]Redondo J.M. (1996) .*Vertical microstructure and mixing in stratified flows.* Advances in Turbulence VI. Eds. S. Gavrilakis et al. 605-608.